Current Optics and Photonics
Vol. 1, No. 3, June 2017, pp. 214-220

ISSN: 2508-7266(Print) / ISSN: 2508-7274(Online)
DOI: https://doi.org/10.3807/COPP.2017.1.3.214

Optimization of Tilted Bragg Grating Tunable Filters Based on Polymeric Optical Waveguides

Tae-Hyun Park, Guanghao Huang, Eon-Tae Kim, and Min-Cheol Oh*

Department of Electronics Engineering, Pusan National University, Pusan (Busan) 46241, Korea

(Received November 18, 2016 : revised March 13, 2017 : accepted March 14, 2017)

A wavelength filter based on a polymer Bragg reflector has received much attention due to its simple structure and wide tuning range. Tilted Bragg gratings and asymmetric Y-branches are integrated to extract the reflected optical signals in different directions. To optimize device performance, design procedures are thoroughly considered and various design parameters are applied to fabricated devices. An asymmetric Y-branch with an angle of 0.3° produced crosstalk less than -25 dB, and the even-odd mode coupling was optimized for a grating tilt angle of 2.5°, which closely followed the design results. Through this experiment, it was confirmed that this device has a large manufacturing tolerance, which is important for mass production of this optical device.

Keywords : Integrated Optics, Tunable wavelength filter, Polymer waveguide devices
OCIS codes : (130.5460) Polymer waveguides; (130.3120) Integrated optics devices; (130.7408) Wavelength filtering devices

I. INTRODUCTION

In a wavelength-division-multiplexed (WDM) optical communication network, tunable wavelength filters are required to filter a certain wavelength among the multiplexed wavelength signals arriving at a destination [1, 2]. Many different technologies based on thin films, Fabry-Perot resonators, or ring resonators have been proposed. A thin-film filter has advantages of thermal stability and good reproducibility; however, it consumes a large amount of thermal tuning power and has slow tuning speed [3-5]. A Fabry-Perot filter has the merit of a wide tuning range; however, multiple wavelength signals could pass if the wavelength varies over the free spectral range (FSR) and a long-term stability is still an issue related to the mechanical actuator [6, 7]. The fiber-optic Bragg grating has advantages of low loss and narrow bandwidth; however, it is bulky and has a relatively small tuning range [8, 9]. The ring resonator filter has a simple structure and it can be integrated easily; however, it has a small tuning range limited by the FSR [10, 11].

The Bragg grating filter, which only reflects a single wavelength, is suitable for WDM optical communication systems due to its narrow bandwidth and flat top passband [12-14]. The Bragg reflectors based on polymer materials have wide wavelength-tuning ranges due to the excellent thermo-optic (TO) effects of the polymer materials [15-18]. However, in a conventional Bragg reflector, since the reflected light returns to the input port, an additional external optical circulator is required to extract the output signal through another path. To achieve low-cost compact tunable filters without using the external circulator, several designs have been proposed for a polymer Bragg reflector in which the input and output ports are separated [19-22]. A device using a Y-branch waveguide and a reflective mirror was proposed as a straightforward solution, but the additional loss was too high [19]. An asymmetric coupler was incorporated along with a Bragg reflector to redirect the reflected light; however, it was difficult to tune the initial crossover state of the coupler [20]. An asymmetric X-junction mode-sorting device was utilized to change the direction of the reflected light [21]. In this device, however,

*Corresponding author: mincheoloh@pusan.ac.kr
Color versions of one or more of the figures in this paper are available online.

a phase controller was necessary to adjust the relative phases of the two reflected waves. In order to overcome the burden of phase control, in our recent work, we used a tilted Bragg grating along with a mode sorting Y-branch [22].

In this study, a tunable polymer wavelength filter based on a tilted grating is analyzed through design and manufacture, and it is determined whether the device has sufficient manufacturing tolerance for mass production. The design of the asymmetric Y-branch optical waveguide structure and the effect of the angle change of the tilted Bragg grating on the device characteristics are investigated. Based on these results, we fabricated devices with different structures over an appropriate range, and confirmed that they have tolerances that are wider than the controllable error range in the device fabrication process.

II. ANALYSIS OF THE MODE EVOLUTION AND COUPLING

The proposed tunable filter consists of a tilted Bragg grating and an asymmetric Y-branch waveguide as shown in Fig. 1. When the input light launched into the narrow waveguide propagates through the asymmetric Y-branch, it goes through an evolution of the mode profile and arrives at the two-mode waveguide in the form of an odd mode. The tilted Bragg grating then reflects the odd mode to the even mode as long as the wavelength matches the Bragg condition. This reflected even mode propagates back to the Y-branch, where it evolves and propagates onto the wide waveguide. The efficiency of mode evolution and the mode coupling between the even and odd modes can be analyzed using the effective-index method (EIM), the overlap integral of perturbed modes, and the beam propagation method (BPM).

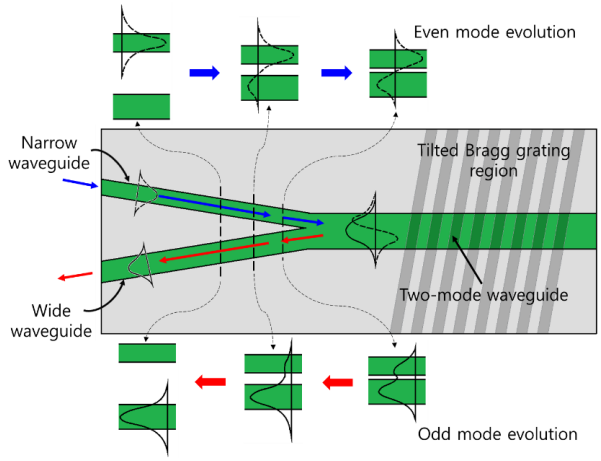

FIG. 1. Schematic structure of a channel-drop wavelength filter consisting of a tilted Bragg reflector and an asymmetric Y-branch. The evolutionary mode profiles along the propagation direction are shown for each cross-section.

2.1. Design of Tilted Bragg Grating

The tilted grating is placed on a two-mode waveguide, which supports both even and odd modes. We use EIM to design the channel-type waveguide. The refractive index of the core and cladding are 1.455 and 1.435, respectively. The thickness of the core layer is 2.5 μm. According to the calculation result shown in Fig. 2, the waveguide should be wider than 4.6 μm to accommodate both even and odd modes.

The mode conversion efficiency between the odd and even modes, η_{oe}, which depends on the tilt angle of the Bragg grating, can be calculated using the following mode-overlapping integration [23],

$$\eta_{oe} = \frac{\int\int \psi_o^*(x,y)\exp[i2\pi x\tan(\theta_t)/\Lambda]\,\psi_e(x,y)dxdy}{[\int\int \psi_o^*(x,y)\psi_o(x,y)dxdy \int\int \psi_e^*(x,y)\psi_e(x,y)dxdy]^{1/2}}. \quad (1)$$

ψ_e and ψ_o are the electric field distributions of the even and odd modes, respectively. The perturbation by a grating with a tilt angle of θ_t and a period of Λ determines the mode conversion efficiency. As shown in Fig. 3(a), for a θ_t of 0°, the two orthogonal modes will not couple and will result in an $\eta_{oe} = 0$. In this case W_t is 7 μm. η_{oe} increases as the grating perturbation effect grows, as θ_t becomes larger, and it reaches a maximum value at an optimum angle. The tilted grating also causes coupling between the two even modes and the two odd modes resulting in a mode conversion efficiency of η_{ee}, and η_{oo}, respectively, as shown in Fig. 3(a). In these results, at an optimum θ_t, η_{oe} becomes the maximum and η_{oo} becomes the minimum. Therefore, for an optimal value of θ_t, if the odd mode is incident on a tilted grating, the reflections will produce only the even mode, and the tilted grating will exhibit the best mode conversion efficiency.

The optimal θ_t is also influenced by the mode profiles, and it decreases when the width of the odd mode increases proportional to the waveguide width. To find the optimal θ_t depending on the width of the two-mode waveguide, W_t, η_{oo} is calculated as a function of θ_t, as shown in Fig. 3(b). The optimal θ_t, as well as the η_{oe}, depends on W_t, as shown in Fig. 3(c) in which θ_t is decreasing and η_{oe} is increasing slightly as W_t increases.

The mode-coupling condition produced by the tilted grating can be described using the *K*-vector diagram. The *z*-component

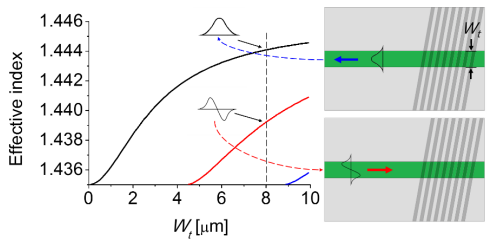

FIG. 2. Effective-index calculation results of the even and odd modes depending on the width of the waveguide. The two modes propagating back and forth through the two-mode waveguides are also shown.

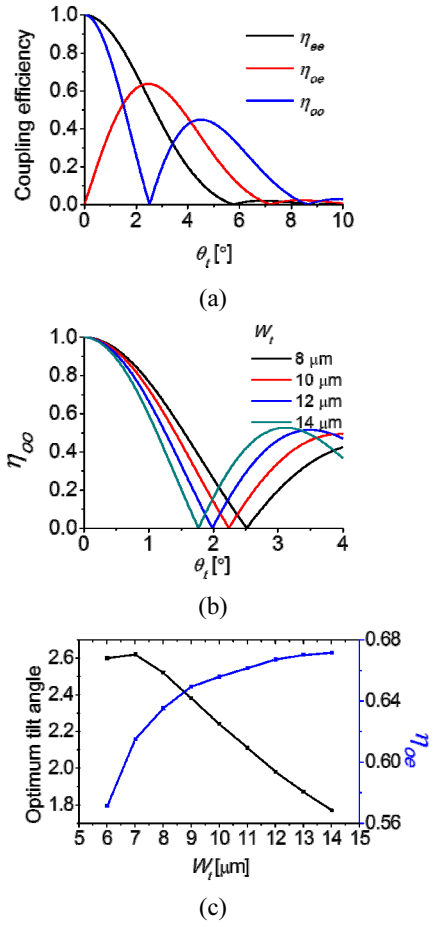

FIG. 3. (a) Mode coupling efficiency as a function of the tilt angle θ_t (for W_t of 7 μm), where η_{oo} becomes minimum at the optimum tilt angle ($\theta_t = 2.52°$); (b) η_{oo} values calculated for various widths of the two-mode waveguide, W_t, in which the optimum tilt angle increases as W_t increases; (c) Optimum tilt angle and η_{oe} calculated as functions of W_t.

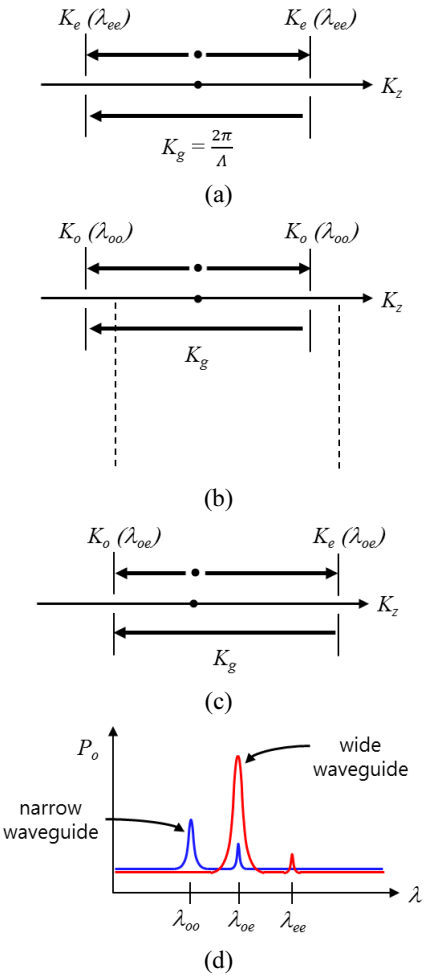

FIG. 4. K-vector diagrams concerning the mode coupling between (a) even and even modes, (b) odd and odd modes, and (c) even and odd modes. The reflection spectral peaks for the three cases of Bragg reflection conditions could be appeared as (d).

of the K-vector and the grating wave vector K_g corresponding to the grating period Λ are presented in Fig. 4. For a wavelength of λ_{ee}, even-even mode coupling occurs as shown in Fig. 4(a), and the even-mode wave vector K_e becomes half of the grating vector, to satisfy the Bragg reflection. For a wavelength of λ_{oo}, the odd mode satisfies the Bragg condition with $K_o(\lambda_{oo}) = \frac{1}{2}K_g$ as shown in Fig. 4(b), where K_o is the odd-mode wave vector. Comparing the two Bragg conditions, because the odd modes have smaller effective indexes than the even modes, λ_{oo} should be shorter than λ_{ee} to satisfy $K_o(\lambda_{oo}) = K_e(\lambda_{ee})$. For a wavelength of λ_{oe}, Bragg reflection occurs between the odd and even modes by satisfying $K_e(\lambda_{oe})+K_o(\lambda_{oe}) = K_g$ as shown in Fig. 4(c). Then, by comparing the even-mode wave-vectors, one can find $K_e(\lambda_{oe}) > K_e(\lambda_{ee})$, such that $\lambda_{oe} < \lambda_{ee}$ while $\lambda_{oe} < \lambda_{oo}$ because $K_o(\lambda_{oe}) < K_o(\lambda_{oo})$. These three cases of Bragg reflection conditions will produce three peaks in the reflection spectra as shown in Fig. 4(d). Because of the modal crosstalk in the asymmetric Y-branch, the reflection spectra measured in the wide and narrow waveguides could contain some spurious peaks.

2.2. Design of Asymmetric Y-branch

In an ideal adiabatic asymmetric Y-branch, to prevent higher order mode excitation, the spatial distribution of modes should change very slowly. 2-D BPM analysis was carried out based on the effective-index profile of the channel waveguide. The width of numerical sampling grid was 0.05 μm, and the widths of the narrow and wide waveguides were taken as variables - W_n and W_w, respectively. The light launched into the narrow waveguide converts to an odd, while the reflected even mode evolves into the wide waveguide, as shown in Fig. 5(a). The crosstalk of mode evolution was calculated as a function of the branch angle θ_b for several combinations of W_n and W_w, as shown in Fig. 5(b). The crosstalk decreased proportional to θ_b. For W_n and W_w of 3 μm and 4 μm, respectively, there were some points

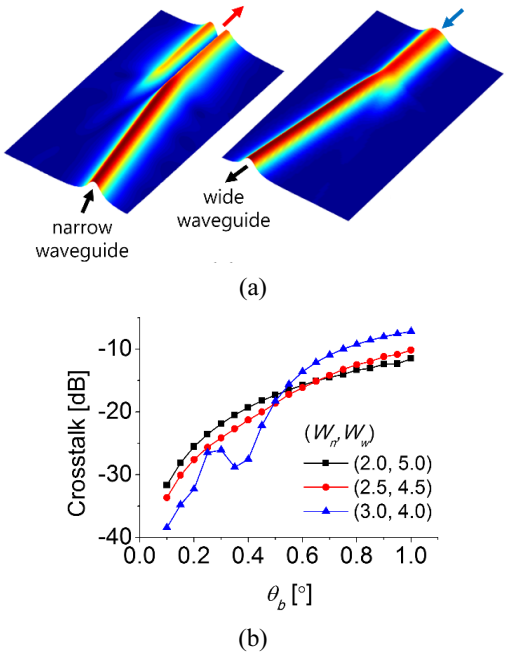

FIG. 5. BPM simulation results of the asymmetric Y-branch waveguide: (a) mode profile evolution of the odd and even modes along the propagation direction, and (b) modal crosstalk produced in the Y-branch calculated as a function of the branch angle θ_b for several combinations of narrow and wide waveguide widths, W_n and W_w.

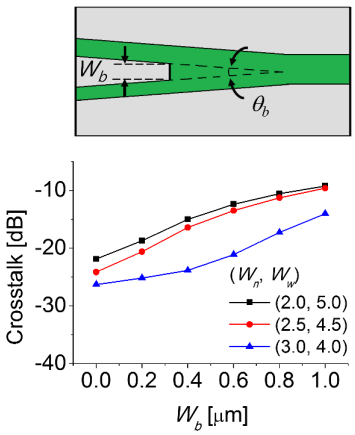

FIG. 6. BPM simulation results to determine the effects of the blunted Y-branch.

where the crosstalk did not decrease monotonically caused by the directional coupling of the higher order modes.

The asymmetric Y-branch has very small angle and produces a blunted tip as shown in Fig. 6, which could affect the mode-evolution efficiency. The modal crosstalk was calculated as a function of the blunt width W_b, for θ_b fixed at 0.3°, as shown in Fig. 6. The crosstalk can be less than -25 dB as long as the W_b stays below 0.4 μm, for W_n, W_w of 3, 4 μm.

III. EXPERIMENTAL RESULTS

3.1. Polymer Waveguide Device Fabrication

ZPU-series polymers by Chemoptics were used for fabricating the tunable wavelength filter. The lower cladding layer was formed by spin coating the ZPU polymer with a refractive index of 1.435 on a silicon wafer. A Bragg grating pattern with a length of 6 mm and a period of 534 nm was fabricated on the lower cladding layer by exposing TSMR photoresist in a two-beam-interference laser set up. It was then transferred onto the lower cladding through oxygen plasma etching. The core layer with a thickness of 2.5 μm was formed by spin coating another ZPU polymer with a refractive index of 1.455. The waveguide pattern was fabricated using AZ5214 photoresist and a 20-nm-thick Cr metal mask. The core layer was then etched by 2.5 μm to define a channel-type waveguide. The upper cladding was formed by spin coating a ZPU polymer of 1.435 refractive index up to a thickness of 8 μm. A thin-film heater was fabricated using a Cr-Au layer (10-100 nm). The fabrication procedure is schematically shown in Fig. 7.

The angle of the tilted grating greatly affects the device performance, and should therefore be controlled precisely. For this purpose, the grating was first inscribed on a wafer placed perpendicular to a flat zone, and then the angle between the grating and the waveguide pattern was adjusted under a mask aligner. In this manner, the θ_t was controllable with an error less than 0.1°. To fulfill the purpose of this work, we need to prepare samples with various coupling conditions for different angles. However, due to the difficulty of changing the θ_t, instead of varying the angle, the widths of the two-mode waveguides were varied, which resulted in the same effect as that explained in Fig. 3.

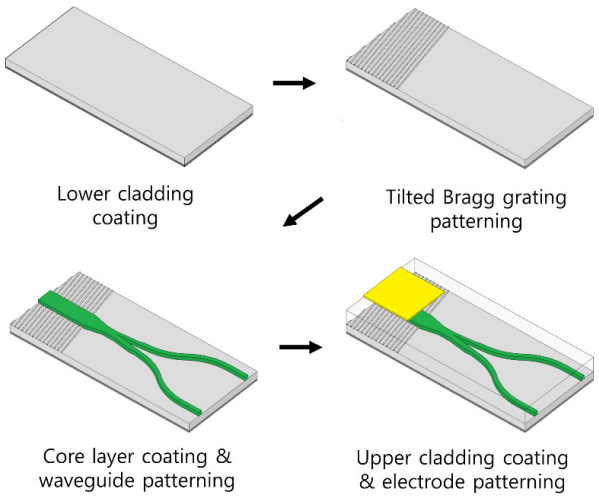

FIG. 7. Schematic fabrication procedure of the proposed polymeric tunable wavelength filter.

3.2. Characterization of the Device

To measure the mode evolution efficiency of the asymmetric Y-branch, a Mach-Zehnder device was prepared by cascading the two asymmetric Y-branches as shown in Fig. 8(a). A distributed feedback (DFB) light source was used to launch a 1550 nm light at the input port, and the two output ports were monitored. A triangular voltage signal was applied to the TO phase modulator. The results of the two devices with θ_b of 0.2° and 0.4° were compared as shown in Fig. 8(b). The devices had a W_n and W_w of 3 μm and 4 μm, respectively. Both devices exhibited less than -20 dB of crosstalk. Although they had different branch angles, the mode-evolution effect was not significantly affected, which means that the device has a high manufacturing tolerance.

The Bragg reflection spectrum was measured using a superluminescent light emitting diode (SLED) light source with a peak wavelength of 1550 nm and a 3-dB bandwidth of 60 nm. The fabricated device had a W_n, W_w, and W_t of 3 μm, 4 μm, and 7 μm, respectively, and the single-mode waveguide had a width of 3.5 μm. The input light launched into the narrow waveguide evolves into the odd mode at the two-mode waveguide and is converted to the even mode through the reflection by the tilted Bragg grating. Then, the reflected light evolves into the wide waveguide. We define this process as narrow-odd-even-wide (NOEW) conversion. On the other hand, some of the light entering a narrow waveguide can be converted to an even mode due to the asymmetric Y-branch crosstalk. It is then produces an odd mode by tilted grating reflection, and propagates toward the narrow waveguide. This process could be called narrow-even-odd-narrow (NEON) conversion. There can also be an narrow-even-even-wide (NEEW) conversion due to the even-even mode reflection from the tilted Bragg grating because η_{ee} is still as high as 50% even for the optimum θ_t. If the θ_t deviates from the optimum θ_t, η_{oo} cannot be zero to produce a narrow-odd-odd-narrow (NOON) conversion. The NOEW and NEEW conversions are detected in the wide waveguide, while the NEON and NOON conversions are

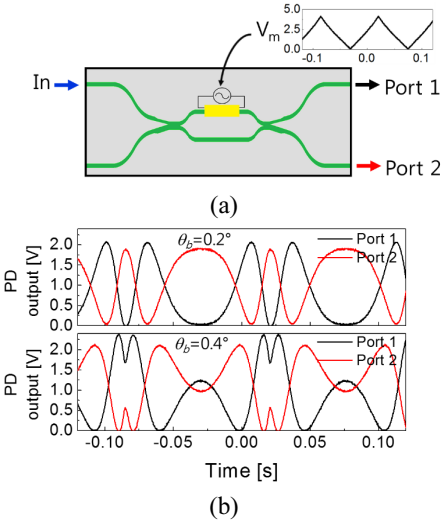

FIG. 8. (a) Mach-Zehnder device formed by cascading the two asymmetric Y-branch devices for measuring the modal crosstalk of the asymmetric Y-branch, and (b) the interference signal obtained by operating the phase modulator, in which the extinction ratio is over 20 dB indicating modal crosstalk as low as -20 dB.

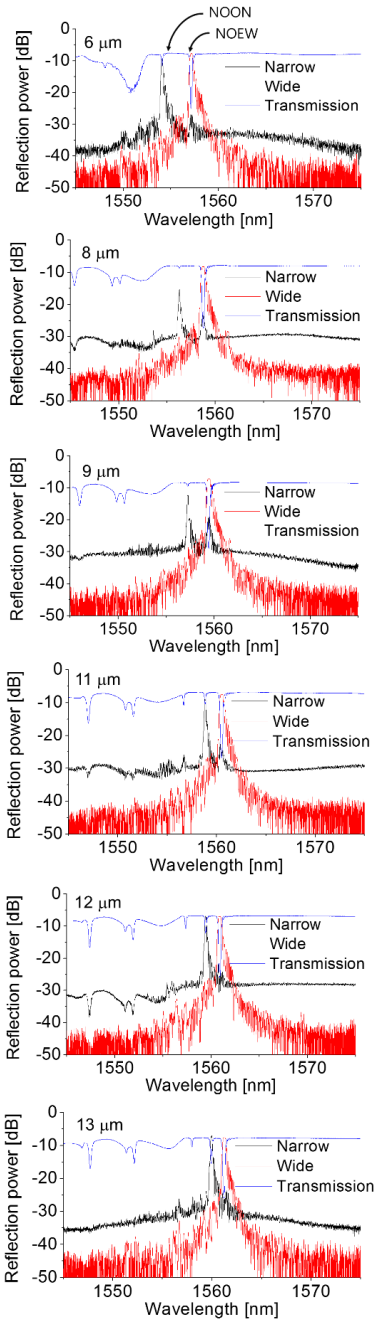

FIG. 9. Reflection spectra of the wavelength filters with various W_ts ranging from 6 μm to 13 μm. For a narrow waveguide input, the output light is measured from the wide waveguide (red line), while another output is measured from the narrow waveguide (black line) using an external circulator. The transmission spectra are also shown for comparison (blue line).

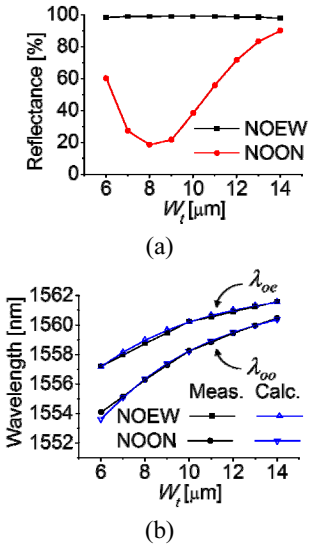

FIG. 10. (a) Reflectivity of NOON and NOEW conversions for various W_ts, and (b) comparison of the design and experimental results of the Bragg reflection peaks for odd–odd coupling and odd–even coupling.

returned back to the input narrow waveguides and an optical circulator is needed to measure their reflection spectra.

As indicated in the previous cascaded Y-branch Mach-Zehnder modulator experiment, because the crosstalk of the mode-sorting waveguide is less than -20 dB, most of the input light launched at the narrow waveguide will be converted into the odd mode. With the θ_t fixed at 2.5°, devices with W_t ranging from 6 μm to 13 μm were prepared for the comparisons with the design results. The reflection spectra were measured as shown in Fig. 9. For the narrow waveguide input, the three reflection peaks explained in Fig. 4(d) were expected. The peaks at λ_{oe} and λ_{oo} could be observed clearly, while the λ_{ee} peak was not found. It is because the asymmetric Y-branch has low crosstalk suppressing the even-mode coupling. In other devices with a poor crosstalk in the Y-branch, the λ_{ee} peak was observed clearly.

As summarized in Fig. 10(a), the magnitudes of the NOEW and NOON peaks were dependent on W_t, and the NOON peak became the lowest for a W_t of 8 μm. In the design, if W_t is 8 μm, the optimum θ_t becomes 2.52°, which is very close to the target angle of the fabricated grating, 2.5°. The peak wavelength of the NOON and NOEW transitions are dependent on W_t as shown in Fig. 10(b). Experimental results determined for various waveguide widths are very close to the design results, which implies that the proposed device can be produced with good repeatability.

IV. CONCLUSION

The complete process of designing a polymer waveguide wavelength filter consisting of a mode alignment waveguide and a tilted Bragg grating has been described and a device has been built to check manufacturing tolerances by carefully evaluating device performance. The characteristics of the tilted Bragg reflector was largely influenced by the tilt angle, which was controllable with an error less than 0.1° in this experiment. The mode-sorting device with a small branch angle produced a blunted branch tip; however, it did not have much effect on the crosstalk in the device. Moreover, the device exhibited wide tolerances for the branch-angle and waveguide-width changes. The reflection spectra from the tilted gratings fabricated on various waveguides with different widths were measured, and were compared with the design results. The mode coupling that occurs in a tilted grating matches very well with the calculated result. Based on these results, we concluded that the proposed wavelength filter has a large manufacturing tolerance and high-yield mass productivity.

ACKNOWLEDGMENT

This work was supported by the National Research Foundation of Korea (NRF) grant funded by the Korea government (MSIP) (2014R1A2A1A10051994), and the ATC project of ChemOptics funded by the Ministry of Knowledge Economy, Korea.

REFERENCES

1. H. Kobrinski and K.-W. Cheung, "Wavelength-tunable optical filters: application and technologies," IEEE. Commun. Mag. **27**, 53-63 (1989).
2. D. Sadot and E. Boimovich, "Tunable optical filters for dense WDM networks," IEEE Commun. Mag. **36**, 50-55 (1998).
3. L. Domash, M. Wu, N. Nemchuk, and E. Ma, "Tunable and switchable multiple-cavity thin film filters," J. Lightwave Technol. **22**, 126-135 (2004).
4. M. Lequime, R. Parmentier, F. Lemarchand, and C. Amra, "Toward tunable thin-film filters for wavelength division multiplexing applications," Appl. Opt. **41**, 3277-3284 (2002).
5. R. Parmentier and M. Lequime, "Substrate-strain-induced tunability of dense wavelength-division multiplexing thin-film filters," Opt. Lett. **28**, 728-730 (2003).
6. B. Yu, G. Pickrell, and A. Wang, "Thermally tunable extrinsic Fabry-Perot filter," IEEE Photon. Technol. Lett. **16**, 2296-2298 (2004).
7. J. S. Milne, J. M. Dell, A. J. Keating, and L. Faraone, "Widely tunable MEMS-based Fabry-Perot filter," J. Micro-electromech. Syst. **18**, 905-908 (2009).
8. G. A. Ball and W. W. Morey, *Tunable Bragg grating fiber filters and their applications* (in Proc. CLEO'97, Baltimore, MD, 1997).
9. A. Iocco, H. G. Limberger, R. P. Salathe, L. A. Everall, K. E. Chisholm, J. A. R. Williams, and I. Bennion, "Bragg grating fast tunable filter for wavelength division multiplexing," IEEE J. Lightwave. Technol. **17**, 1217-1221 (1999).
10. T. Hu, W. Wang, C. Qiu, P. Yu, H. Qiu, Y. Zhao, X. Jiang, and J. Yang, "Thermally tunable filters based on third-order

microring resonators for WDM applications," IEEE Photon. Technol. Lett. **24**, 524-526 (2012).
11. X. Zheng, I. Shubin, G. Li, T. Pinguet, A. Mekis, J. Yao, H. Thacker, Y. Luo, J. Costa, K. Raj, J. E. Cunningham, and A. V. Krishnamoorthy, "A tunable 1×4 silicon CMOS photonic wavelength multiplexer/demultiplexer for dense optical interconnects," Opt. Express **18**, 5151-5160 (2010).
12. M.-C. Oh, M.-H. Lee, J.-H. Ahn, H. J. Lee, and S.-G. Han, "Polymeric wavelength filters with polymer gratings," Appl. Phy. Lett. **72**, 1559-1561 (1998).
13. C. Riziotis and M. N. Zervas, "Design considerations in optical add/drop multiplexers based on grating-assisted null couplers," J. Lightwave Technol. **19**, 92-104 (2001).
14. J. M. Castro, D. F. Geraghty, B. R. West, and S. Honkanen, "Fabrication and comprehensive modeling of ion-exchanged Bragg optical add-drop multiplexers," Appl. Opt. **43**, 6166-6173 (2004).
15. M.-C. Oh, W.-S. Chu, J.-S. Shin, J.-W. Kim, K.-J. Kim, J.-K. Seo, H.-K. Lee, Y.-O. Noh, and H.-J. Lee, "Polymeric optical waveguide devices exploiting special properties of polymer materials," Opt. Commun. **362**, 3-12 (2016).
16. Z. Zhang and N. Keil, "Thermo-optic devices on polymer platform," Opt. Commun. **362**, 101-114 (2016).
17. Z. Zhang, D. D. Felipe, W. Brinker, M. Kleinert, A. M. Novo, M. Moehrle, C. Zawadzki, and N. Keil, "C/L-band colorless ONU based on polymer bi-directional optical subassembly," IEEE J. Lightwave. Technol. **33**, 1230-1234 (2015).
18. Y.-O. Noh, H.-J. Lee, J. J. Ju, M.-S. Kim, S. H. Oh, and M.-C. Oh, "Continuously tunable compact lasers based on thermo-optic polymer waveguides with Bragg gratings," Opt. Express **16**, 18194-18201 (2008).
19. S.-H. Park, J.-K. Seo, J-O Park, H.-K. Lee, J.-S. Shin, and M.-C. Oh, "Transmission type tunable wavelength filters based on polymer waveguide Bragg reflectors," Opt. Commun. **362**, 96-100 (2016).
20. W.-C. Chuang, Y.-T. Huang, H.-C. Lin, and A.-C. Lee, "Fabrication of an asymmetric Bragg coupler-based polymeric filter with a single-grating waveguide," Opt. Express **19**, 10776-10788 (2011).
21. J.-S. Shin, T.-H. Park, W.-S. Chu, C.-H. Lee, S.-Y. Shin, and M.-C. Oh, "Tunable channel-drop filters consisting of polymeric Bragg reflectors and a mode sorting asymmetric X-junction," Opt.Express **23**, 17223-17228 (2015).
22. T.-H. Park, J.-S. Shin, G. H., W.-S. Chu, and M.-C. Oh, "Tunable channel drop filters consisting of a tilted Bragg grating and a mode sorting polymer waveguide," Opt. Express **24**, 5709-5714 (2016).
23. J. M. Castro, D. F. Geraghty, S. Honkanen, C. M. Greiner, D. Iazikov, and T. W. Mossberg, "Optical add-drop multiplexers based on the antisymmetric waveguide Bragg grating," Appl. Opt. **45**, 1236-1243 (2006).